DOI: 10.61782/fa.2023.0209

forum acusticum 2023

NONRECIPROCAL VIBRATION TRANSMISSION USING DISLOCATED POSITION FEEDBACK

Srećko Arandia-Krešić[1*] **Neven Alujević**[1] **Daniel Krivačić**[2] **Aleksandar Sušić**[1]

[1] Faculty of Mechanical Engineering and Naval Architecture, University of Zagreb, Croatia
[2] Technical University of Munich, Munich, Germany

ABSTRACT

This paper examines absolute position feedback using dislocated sensor-actuator pairs to design and implement an active metamaterial cell for non-reciprocal vibration transmission. It has been shown previously that by using dislocated sensor-actuator pairs to implement absolute velocity feedback, a stable and robust nonreciprocal vibration transmission can be achieved. In contrast to other active approaches, which typically induce narrowband non-reciprocity, the dislocated transducer pair methodology induces a broadband non-reciprocity. However, the passive cell before control must be carefully designed to mitigate instability due to the lack of collocation between sensor-actuator pairs. Furthermore, with absolute velocity feedback, the reciprocity loss decreased as the frequency decreased. Therefore, the achievable non-reciprocity was relatively weak at low frequencies where the error velocity signals were fairly small. It is therefore of interest to consider pure absolute position feedback, where strong quasi-static and low-frequency error signals could potentially induce a large nonreciprocity also at low frequencies. Therefore, in this study comprehensive stability and performance analyses of the absolute position feedback using dislocated sensor-actuator pairs are carried out both theoretically and experimentally. The difference in the vibration transmissibility in the two opposite directions obtained experimentally amounts to quite spectacular 30 dB in the frequency range between 30-1000Hz.

Keywords: dynamic reciprocity, active metamaterials, stability of active control systems, performance of active control systems, absolute position feedback

1. INTRODUCTION

There has been an intense surge of interest in active metamaterials in the last decade in various areas of physics and engineering [1-3]. In particular, active metamaterials exhibit previously unseen properties on the macro-scale, which cannot be found in natural materials. For example, Kramers-Kronig relations bound the dispersion properties of passive, linear time-invariant (LTI) media, which limits the spectral range of the target effective properties. Furthermore, the efficiency of passive metamaterials is hindered by losses, as there is no compensation mechanism for potentially undesirable, yet inherent energy dissipation due to, for example, structural damping [1]. By providing energy input into the material these losses can be compensated for, which enables a whole new spectrum of exotic wave phenomena. In this paper, the particular phenomenon in focus is the non-reciprocal vibration transmission in mechanical structures, which, using the proposed methodology, is achievable regardless of their linear elastic nature. The reciprocity principle in structural dynamics states that if points of excitation and response of a structure are switched, the output quantity will not change. This is often a useful property, but its disruption can also be of interest. Non-reciprocal vibration transmission is interesting for applications such as invisible acoustic sensors [4], acoustic cloaking devices [5], vibration isolation [6],

[*] ***Srećko Arandia-Krešić***: *sarandia@fsb.hr*

autonomous and active guiding of sound beams [7], or full duplex sound communication where acoustic waves can be transmitted and received from the same transducer on the same frequency channel [8]. Approaches to cancel the reciprocity in vibroacoustics have mostly relied on non-linear effects, [9] that, unfortunately, are accompanied by unwanted features such as bulky structures, high power consumption and large signal distortion. Recently, a new concept emerged that proved in theory and practice to be exceptionally efficient at breaking the reciprocity [6, 10] of vibroacoustic structure. It was observed that by using the so-called non-collocated sensor-actuator pairs forming velocity feedback loops, the amplitudes of two transfer mobility functions for two opposite directions of propagation through the active metastructure showed to be different along the wide frequency band. This indicates a strong loss of reciprocity. Furthermore, this difference was increasing as the frequency increased. The static reciprocity, however, remained intact due to the velocity error signal used that vanishes as the frequency tends to zero. On the other hand, if position, rather than velocity is measured, the error signal would not vanish, but instead, increase as frequency tends to zero. This article is therefore dedicated to the absolute position feedback control with dislocated sensor-actuator pairs, and discusses ways to ensure stability and convincing control performance for such a sensor-actuator arrangement.

2. THEORETICAL CONSIDERATIONS

2.1 Negative position feedback

Both mentioned control concepts are briefly introduced next. Fig. 1a) shows a 2-degree-of-freedom (2DOF) mechanical system. Each is modelled as a single-degree-of-freedom (SDOF) oscillator. Each of the two oscillators approximates a potentially more complicated distributed parameter structure through its fundamental vibration mode, like, for example, in references [11, 12]. The first substructure (brown) is modelled through mass m_1 and spring k_1 whereas the second one (pink) is modelled through mass m_2 and spring k_3. A velocity sensor is placed on the second substructure operating within a feedback loop encircled in yellow colour. The velocity signal is augmented by a proportional gain and fed back to a force actuator reacting between the first and the second substructure. This kind of arrangement induces a strong reciprocity loss when comparing the response of mass m_2 to forcing applied at mass m_1 to the response of mass m_1 to forcing exerted at mass m_2.

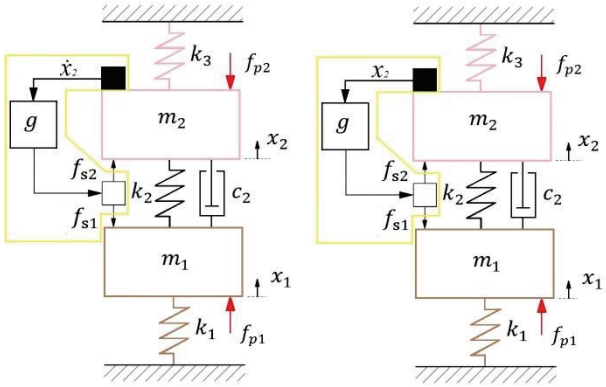

Figure 1. Model of a 2DOF metamaterial cell with 2 active schemes: a) velocity feedback, b) position feedback.

When represented as amplitudes of the two corresponding transfer mobility functions, it becomes clear that the reciprocity loss increases with frequency [6, 10]. Therefore, at low frequencies, the amplitudes are identical, as if the feedback loop is not active. In theory, this problem could be circumvented by using position feedback in order to ensure a large low-frequency error signal. This kind of control architecture is shown in Fig. 1b). However, a position sensor and a force actuator are not dual, that is, the error position and the control force are not complementary in terms of mechanical power. This may cause both stability and control performance problems in addition to those expected due to the dislocated sensor-actuator arrangement.

Attention is now turned to Fig. 1b). The two substructures are coupled through a coupling spring k_2 and a dashpot c_2. The dashpot c_2 is used in order to consider the relatively large air-gap damping which is typical for coil-magnet actuators [13], whereas the damping of the two uncoupled substructures is assumed negligible for simplicity. The error position sensor is mounted at the second substructure modelled by mass m_2 and spring k_3. The control actuator exerts two secondary (control) force components proportional to the error position signal: an action, f_{s2}, and a reaction, f_{s1}. The action control force component is collocated with the position sensor whereas the reaction control

force component is dislocated from the sensor (see Fig. 1). The mathematical model of the lumped parameter system is described with

$$\mathbf{M}\mathbf{x} + \mathbf{C}\mathbf{x} + \mathbf{K} = \mathbf{f}, \tag{1}$$

where $\mathbf{M}$, $\mathbf{C}$ and $\mathbf{K}$ are mass, damping and stiffness matrices, respectively, $\mathbf{x}$ is the position vector, $\mathbf{x} = [x_1 \quad x_2]^T$ and $\mathbf{f}$ is a vector of primary excitation, $\mathbf{f} = [f_{p1} \quad f_{p2}]^T$. With such a scheme, the control law,

$$f_{s1} = gx_2, f_{s2} = -gx_2, \tag{2}$$

can be written directly into the stiffness matrix in the following way, making it diagonally asymmetric:

$$\mathbf{K} = \begin{matrix} k_1 + k_2 & -k_2 - g \\ -k_2 & k_2 + k_3 + g \end{matrix}. \tag{3}$$

This effectively induces asymmetry in the dynamic stiffness matrix $\mathbf{S} = \mathbf{M}s^2 + \mathbf{C}s + \mathbf{K}$, and in its inverse, $\mathbf{S}^{-1}$ which is the matrix of the systems frequency response functions (FRF) [10]. The variable $s = \mathrm{j}\omega$ is the Laplace variable, where $\mathrm{j} = \sqrt{-1}$ represents the imaginary unit and ω is the frequency. In such a way, the displacement vector can be calculated as:

$$\mathbf{x} = \mathbf{S}^{-1}\mathbf{f}. \tag{4}$$

The velocity vector can be calculated as:

$$s\mathbf{x} = s\mathbf{S}^{-1}\mathbf{f} = \mathbf{Q}\mathbf{f}, \tag{5}$$

where $\mathbf{Q}$ is the diagonally asymmetric system mobility matrix. For example, the velocity response of the second substructure, $\dot{x}_2 = Q_{2,1}f_{p1}$, due to the primary forcing at the first substructure, f_{p1}, is now different from the response of the first structure, $\dot{x}_1 = Q_{1,2}f_{p2}$, due to the forcing at the second substructure f_{p2}. Therefore, the two transfer mobilities, $Q_{1,2}$ and $Q_{2,1}$, of the closed-loop system shown in Fig. 1b), are compared in order to quantify the reciprocity loss.

2.1.1 Stability

In order to discuss the stability of the feedback loop, Routh-Hurwitz stability criterion is used first. According to this criterion, a necessary condition for stability is that all the coefficients of the characteristic equation are of the same sign. Further to that, all determinants of the Routh-Hurwitz array must be positive. After calculating the coefficients of the characteristic equation and the determinants of the Routh-Hurwitz array, the necessary condition for stability of the system reads:

$$\frac{k_1}{m_1} \leq \frac{k_3}{m_2}. \tag{6}$$

It can be seen from inequality (6) that in order for the active system to be stable for all positive feedback gains, $g \geq 0$, the natural frequency of the first substructure (brown spring-mass system in Fig. 1) must be *lower* than the natural frequency of the second substructure (pink spring-mass in Fig. 1). This implies that by carefully choosing parameters of the passive system before control, unconditional stability can be accomplished despite the dislocated sensor-actuator configuration. Note that collocated sensor-actuator configuration is normally preferred for its beneficial stability properties [14]. It is interesting to note that the stability condition on the passive structure before control is opposite of that calculated in ([6], [10]) considering the absolute velocity feedback control scheme like the one shown in Fig. 1a). In other words, if absolute velocity feedback is considered instead of the absolute position feedback, then the natural frequency of the first substructure must be *higher* than the natural frequency of the second substructure.

If negative feedback gains are considered ($g \leq 0$) then the feedback loop implements positive position feedback. In this case, if the passive system properties satisfy Eqn. 6, the unconditional stability is not possible and there exists a maximum stable feedback gain. Fig. 2 illustrates the range of positive and negative stable feedback gains for the system shown in Fig. 1b) assuming that the passive system properties satisfy Eqn. 6. Note that positive feedback is much more difficult when using velocity error signals, because of inevitable stability issues with positive velocity feedback.

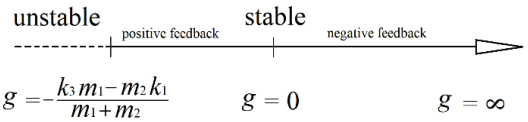

Figure 2. Theoretical stability conditions for positive and negative position feedback gains for the system in Fig. 1b).

The stability of the feedback loop can be further studied by employing the Nyquist stability criterion which enables to conveniently consider relative stability properties such as the gain and the phase margins. The mechanical parameters of the system are shown in Tab. 1. As $m_1 > m_2$ and $k_3 > k_1$, Eqn. 6 is satisfied, and the unconditional stability is guaranteed for g>0. This means that arbitrarily large positive feedback gains may be used without inducing an unstable response. Indeed, it can be seen in the Nyquist plot in Fig. 3, solid line, that the locus of the sensor-actuator open-loop Frequency Response Function (FRF) can never cross the negative real axis.

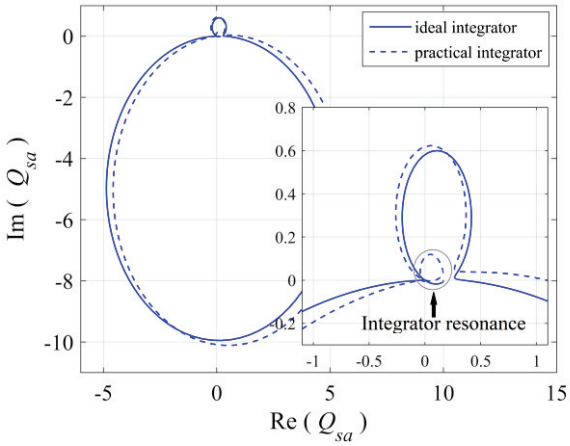

Figure 3. The theoretical sensor-actuator open-loop FRF for the absolute position feedback: a) ideal double integrator (solid line), and b) real double integrator (dashed line).

Table 1 Parameters of the system

m_1 (kg)	m_2 (kg)	k_1 (N/m)	k_2 (N/m)	k_3 (N/m)	c_2 (Ns/m)
0.0808	0.0485	40050	2750	137150	1.4

This means that there can be no open-loop zeros in the right hand-side of the complex plane. However, this is true only if ideal sensor-actuator transducers are assumed. The error position signals in practice can be obtained by double integration of standard accelerometer signals. The integrator in this study is realised by using a combination of a second order low-pass Butterworth filter in series with a first order high-pass filter having a 5 Hz cut-off frequency. The two filters add additional poles to the sensor-actuator open loop FRF. As a result, the Nyquist locus is rotated in the counter-clockwise direction in comparison with the locus assuming an ideal double integrator (Fig. 3, solid line vs. dashed line). As a result, the closed-loop system is no longer unconditionally stable since there is a crossing of the Nyquist locus over the negative reals axis due to the integrator resonance (Fig. 3, zoomed plot area).

2.1.2 Performance

The comparison of the amplitudes of the closed-loop transfer mobilities, $|Q_{2,1}|$ vs. $|Q_{1,2}|$ is shown in Fig. 4 as an illustration of the achievable reciprocity loss.

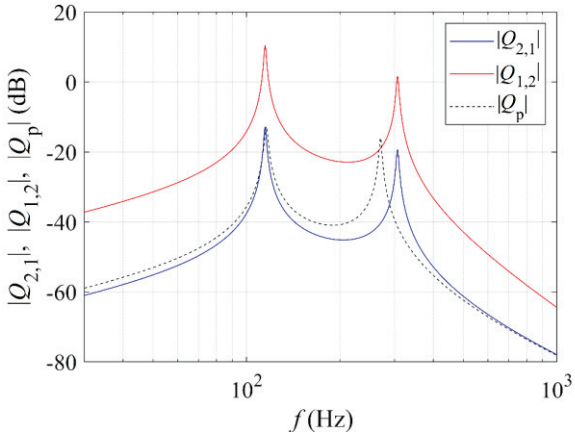

Figure 4. The loss of reciprocity induced by a negative position feedback control with g = 40000 N/m.

As can be seen in the figure, the simulated difference between the two amplitudes assuming an idealised double-integrator is around 24 dB at 30 Hz for the feedback gain of 40000 N/m. This value of the feedback gain is similar to the spring stiffness k_1 (see Tab. 1). The reciprocity loss decreases as the frequency increases due to the mass law which dictates a roll-off of 40 dB per decade of the error signal with increasing the frequency. One mobility function ($Q_{1,2}$) is boosted by switching the active control on, while the other

one ($Q_{2,1}$) slightly decreases. This decrease can also be larger depending on the parameters of the passive system before control. The increase of the feedback gain separates the two resonance frequencies of the closed-loop system more and more, since the fundamental resonance frequency shifts downwards while the second resonance shifts upwards. This is associated with the negative position feedback, which has the effect of adding to the stiffness of the existing passive springs, see the stiffness matrix in Eqn. 3.

2.2 Positive position feedback

2.2.1 Stability

However, one may go beyond the negative position feedback ($g \geq 0$) and consider positive position feedback ($g<0$). It can be shown by using the Routh-Hurwitz stability analysis that the unconditional stability for positive position feedback cannot be obtained if Eqn. 6 is respected, even if an idealised double-integrator is assumed. Instead, stability is guaranteed under the condition:

$$g \geq \frac{k_1 m_2 - k_3 m_1}{m_1 + m_2}, \tag{7}$$

see also Fig. 2. Despite the conditional stability of the feedback loop, this is also an interesting control strategy to induce the non-reciprocal response. However, with the positive position feedback the stability of the system may become corrupted by the frequency response of realistic integration filters. This can be seen by considering the sensor-actuator open-loop FRFs shown in Fig. 5. In contrast to the situation with the negative position feedback (Section 2.1), where the counter-clockwise rotation induced by the realistic integrators in comparison with the ideal integrators does not jeopardise the stability, with the positive position feedback this counter-clockwise rotation is detrimental. This can be seen in Fig. 5 whereby comparing the solid line (ideal integrator) to the dashed line (realistic integrator) one observes a reduction of the phase margin due to the use of the realistic integrator. This problem may be circumvented by adding a low-pass filter with a higher cut-off frequency to rotate the locus of the sensor-actuator open loop FRF back in the clockwise direction (Fig. 5, dash-dotted line). However, this rotation must not be excessive. Otherwise, the active stiffness approach turns into active damping. Therefore the cut-off frequency of this additional low-pass filter must not be too low (1 kHz was used in the present example).

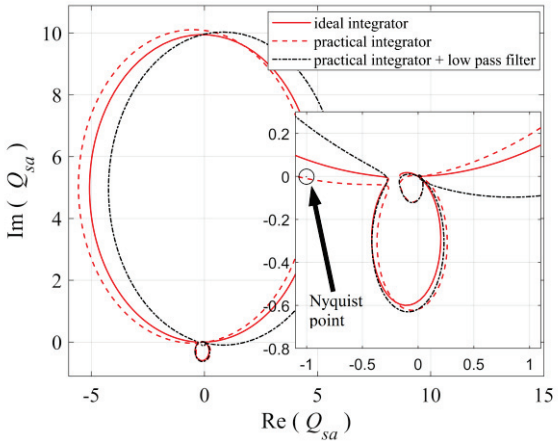

Figure 5. Sensor-actuator open-loop FRF assuming a positive position feedback: ideal double integrators (solid line), practical double integrators (dashed line), practical double integrators with a LP-filter (dash dotted line).

2.2.2 Performance

The control performance using the positive position feedback can be assessed through the results shown in Fig. 6. A large difference of about 25 dB in the amplitudes of the two transfer mobilities $Q_{1,2}$ and $Q_{2,1}$ is accomplished when using the feedback gain of g = -40000 N/m. Even though the absence of reciprocity is evident, it is noticeable that in contrast to all previous cases studied, the amplitudes of the two mobilities are now both increased with respect to the passive case. Also, in contrast to the negative position feedback, an increase of the feedback gain merges the resonant frequencies together. This is because the control loop gain is now subtracted from the passive spring stiffnesses which reduces the total stiffness of the system, see again Eqn. 3, stiffness matrix. The two FRFs are characterised by a damped response at the second resonance frequency which can be attributed to the 1 kHz low-pass filter used. This is because the position feedback gradually turns into velocity-like feedback as the frequency approaches and surpasses the cut-off frequency of the filter. This also widens the frequency range in which the loss of reciprocity is relatively high. The filtered position feedback

effectively establishes a proportional-integral (PI) controller. The application of this kind of controller is an interesting direction for future research.

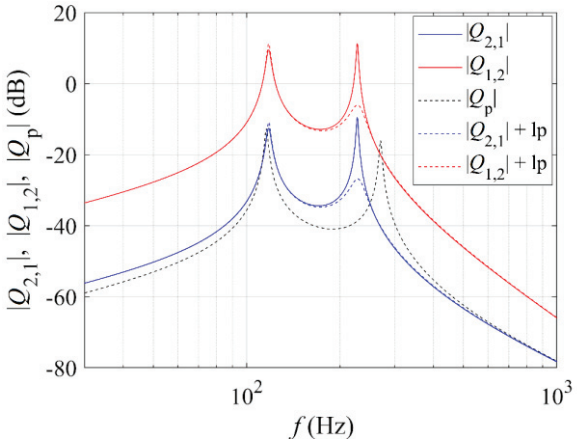

Figure 6. The loss of reciprocity induced by a positive position feedback control with g = -40000 N/m.

3. EXPERIMENTAL VALIDATION

3.1 Experimental test rig

The experimental setup is shown in Fig. 7. The setup mimics the lumped parameter model in that the masses are realised by concentrating fairly rigid lumps of material whereas the stiffnesses are realised by lightweight flexible straight or curved beam elements. Masses m_1 and m_2 are mimicked by blocks connected via leaf springs (stiffnesses k_1 and k_3) to a massive frame which is mounted on a rigid foundation. These blocks of material are connected to each other by a leaf spring (stiffness k_2). A significantly greater mass and stiffness of the blocks in comparison to the masses and stiffnesses of the leaf springs ensure that the first two natural frequencies, as well as their corresponding vibration modes, for the most part agree with ones that would be calculated assuming that the springs do not possess inertia and that the blocks were rigid. Accelerometers are used to obtain the error position signal and to measure the characteristic frequency response functions in the two opposite directions. The control actuator is in the middle of the setup (grey rectangle), whereas the primary excitations are provided by the peripheral actuators (blue rectangle). Note that mass m_1 and stiffness k_3 are larger than their counterparts m_2, k_1 to ensure stability, in accordance with Eqn. 6.

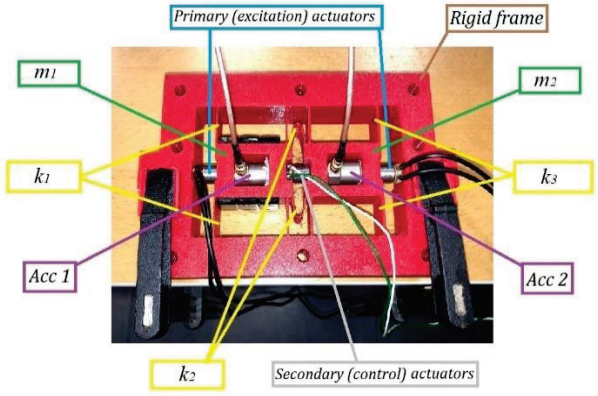

Figure 7. 3D printed experimental test rig of the 2DOF metamaterial cell.

3.2 Experimental results for negative position feedback

The Nyquist plot of the open-loop sensor-actuator FRF, assuming negative position feedback is presented with the solid blue line in Fig. 8. The open-loop gain is set so that the locus goes exactly through the Nyquist point (-1+0j). It can be seen when comparing with the theoretical results shown in Fig. 3, dashed line, that the theory and the experiment qualitatively agree. There are, however, quantitative differences that can be attributed to the fact that the experimental setup is a distributed parameter structure. Therefore, additional smaller circles can be seen which correspond to higher-order resonances at higher frequencies. The amplitudes of the two characteristic FRFs are shown in Fig. 9. The first is obtained by measuring the velocity of the right-hand side lumped mass due to the voltage by the left primary actuator ($Q_{2,1}$) and the second is obtained by measuring the velocity of the left-hand side lumped mass due to the voltage by the right primary actuator ($Q_{1,2}$). These two characteristic FRFs are at low frequencies nearly proportional to the two transfer mobilities ($Q_{2,1}$ and $Q_{1,2}$) discussed in Section 2 since the influence of the coil inductance is only significant for the particular type of the actuator used above the frequency of about 2.4 kHz. Around 25dB difference is achieved between the two amplitudes in a broad band of frequencies. However, this difference gradually reduces as the frequency increases due to the decrease of the error signal with increasing the frequency.

3.3 Experimental results for positive absolute position feedback

As already shown in Section 2.2.1, a much larger stability margin is enabled by adding a low-pass filter with a cut-off frequency at 1 kHz, which results in the

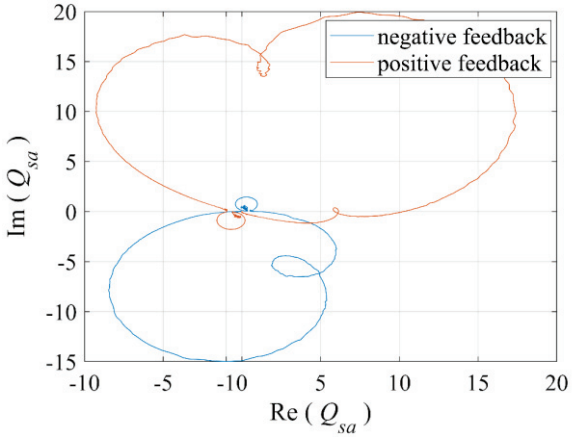

Figure 8. Experimental results for sensor-actuator open-loop FRF assuming positive (red solid line) position feedback with 1 kHz LP filter and negative (blue solid line) position feedbacks.

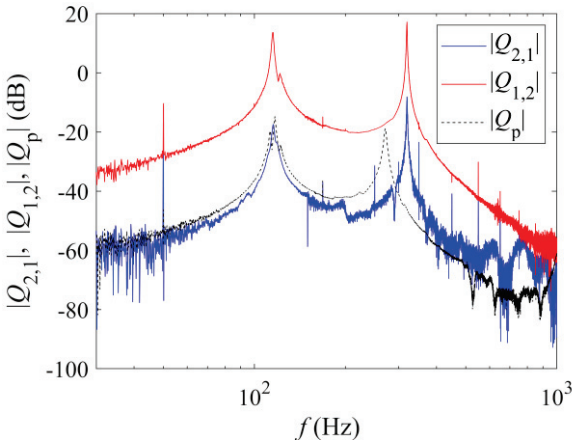

Figure 9. Experimental response of the negative position feedback.

Nyquist contour of the sensor-actuator FRF moving clockwise, thereby enabling larger feedback gains, see Fig. 8. When it comes to the performance of the active control system, the damping effect around the second resonance is also confirmed experimentally. This is due to the application of the low-pass filter as already discussed in Section 2.2.1. When comparing the reciprocity loss and the resonance frequency shifts (Fig. 10), the experimental results are qualitatively similar to the simulation results. The reciprocity loss at 30 Hz is around 30 dB and gradually decreasing with the increase in frequency.

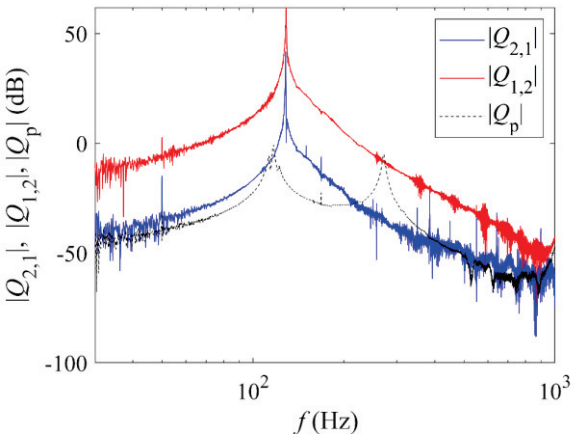

Figure 10. Experimental response of the positive position feedback.

4. CONCLUSION

In this paper, an active metamaterial cell for non-reciprocal vibration transmission using position feedback with dislocated sensor-actuator pairs is discussed. The passive and active response of the metamaterial cell is first simulated using a 2DOF lumped parameter model. In contrast to earlier considerations, both positive and negative feedback of the position signal are analysed. It is shown that theoretical unconditional stability can be achieved despite the dislocated sensor-actuator configuration. This is possible if the passive system before control is tuned such that the natural frequency of the uncoupled second substructure is larger than the natural frequency of uncoupled first substructure. This is exactly opposite to the stability condition when using absolute velocity feedback using dislocated sensor-actuator pairs [10], [15]. This may pose a challenge in case a combination of velocity and position feedback is considered to further widen the frequency range where the reciprocity is cancelled. However, even with pure absolute position feedback the reciprocity loss obtained is quite large (20-30 dB) and broadband (30-1000 Hz). The experimental analysis confirms the theoretical results and the experimentally

obtained loss of reciprocity at low frequencies is of order of 30 dB.

5. ACKNOWLEDGMENTS

The Croatian Science Foundation HRZZ-IP-2019-04-5402 (DARS) support is gratefully acknowledged.

6. REFERENCES

[1] F. Zangeneh-Nejad, R. Fleury, “Active times for Acoustic Metamaterials”, Rev. Phys. vol. 4, no. 100031, 2019.

[2] L. Sirota, A. M. Annaswamy, “Active wave suppression in the interior of a one-dimensional domain”, Automatica, vol. 100, pp. 403-406, 2019.

[3] A. Marzani, “Prediction of pulse dispersion in tapered waveguides”, NDT & E International, vol. 43, pp. 265-271, 2010.

[4] R. Fleury, D. Sounas, A. Alu, “An invisible acoustic sensor based on parity-time symmetry”, Nat. Commun., vol. 6, pp. 1-7, 2015.

[5] C. House, J. Cheer, S. Daley, “An experimental investigation into active structural acoustic cloaking of a flexible cylinder”, Appl. Acoust, vol. 170, no. 107436, 2020.

[6] N. Alujević, “The absence of reciprocity in active structures using direct velocity feedback”, Journal of Sound and Vibration, vol. 438, pp. 251-256, 2019.

[7] L. Sirota, F. Semperlotti, A. M. Annaswamy, “Tunable and reconfigurable mechanical transmission-line metamaterials via direct active feedback control”, vol. 123, pp. 117-130, 2019.

[8] J. Tan, J. Cheer, S. Daley, “Realisation of nonreciprocal transmission and absorption using wave-based active noise control”, JASA Express Lett, no 054801, 2022.

[9] B. I. Popa, S. A. Cummer, “Non-reciprocal and highly nonlinear active acoustic metamaterials”, Nature Communications, vol. 5, no. 3398, 2014.

[10] M. Jalšić, N. Alujević, T. Garma, I. Čatipović, M. Jokić, H. Wolf, “An active metamaterial cell concept for nonreciprocal vibroacoustic transmission”, Mechanical Systems and Signal Processing, vol. 186, no. 109829, 2023.

[11] A Caiazzo et al, “Active control of turbulent boundary layer sound transmission into a vehicle interior”, J. Phys: Conf. Ser. 744 012026, 2016.

[12] M. Perez, S. Chesne, C. Jean-Mistral, K. Billon, R. Augez, C. Clerc, “A two degree-of-freedom linear vibration energy harvester for tram applications”, Mechanical Systems and Signal Processing, vol 140, 2020.

[13] Q. Chen, L. Li, M. Wang, L. Pei, “The precise modelling and active disturbance rejection control of voice coil motor in high precision motion control system”, Applied Mathematical Modelling, vol. 9, pp. 5936-5948, 2015.

[14] G. J. Balas and J. C. Doyle, "Collocated versus Non-collocated Multivariable Control for Flexible Structure," American Control Conference, pp. 1923-1928, 1990.

[15] N. Alujević, H. Wolf, P. Gardonio, I. Tomac, “Stability and performance limits for active vibration isolation using blended velocity feedback”, Journal of Sound and Vibration, vol. 330, pp. 4981-4997, 2011.